CHAPTER 4

RESULTS AND DISCUSSION (PART I):

Al - OXIDES REINFORCED DENTAL PORCELAINS

In this chapter, the results are presented of the investigation of both Al_2O_3 and Al_2O_3-M_xO_y reinforced dental porcelain systems. Chemical composition, microstructure and mechanical properties relationships are brought out and discussed in terms of phase formation, densification and mechanical properties. Attention is first paid to the porcelain ceramics, before moving on to the Al_2O_3 reinforced porcelain systems.

4.1 Dental Porcelain Ceramics

The purpose of this section was to fabricate dental porcelain ceramics from Thailand's raw materials and to examine the relationships between composition, microstructure and mechanical properties of the dental ceramics. Effects of sintering conditions (i.e. dwell time and heating/cooling rates) on mechanical properties of each dental porcelain compositions are given in Table 3.5. In this work, it is seen that the optimum dwell time and heating/cooling rates for the optimum mechanical properties of each composition were found to be at 3 min and 50 ^oC/min, respectively (Table 4.1). In general, flexural strength, fracture toughness and hardness values range from 57-83 MPa, 0.92-1.24 GPa and 3.03-3.21 MPa.$m^{0.5}$, respectively. Maximum flexural strength and hardness values of 83.4 MPa and 1.01 GPa were found in **D11**. Whilst **D3** exhibits the maximum fracture toughness value of 1.24 MPa.$m^{0.5}$. Evidently, the high-quartz compositions exhibit better hardness and strength properties, while high-

feldspar compositions show larger fracture toughness values [133]. This result clearly indicates the effects of different constituents on the mechanical properties. More importantly, it should be noted that these values are slightly higher than those of specifications required by ISO 6872 [122]. The reasons for these higher values are not very well understood, but could be attributed to mechanisms caused by different raw materials [134,135]. However, this speculation requires further investigation. Not surprisingly, a common feature of all ceramics investigated here is the presence of a significant volume fraction of a glassy phase. SEM micrograph shown in Fig. 4.1 revealed pores as dark regions and nanorods (∅ ~ 50-200 nm) of mullite crystals (Fig. 4.2) growing in the glassy matrix phase. Cracks were seen within quartz grain. These cracks are probably formed by release of microstress within the quartz grains (arrowed) and the surrounding glassy phase resulting from the large thermal expansion coefficient difference between the crystalline quartz ($\alpha \approx 23 \times 10^{-6}$ K^{-1}) and glassy phase ($\alpha \approx 3 \times 10^{-6}$ K^{-1}) in the temperature range 20-750 ^{o}C. This observation is in good agreement with other works. [136-138].

Table 4.1 Average (and standard deviation) of physical and mechanical properties of various dental porcelains.

Sample code	Physical properties		Mechanical properties*		
	Bulk density (g/cm^3)	Total porosity (%)	Flexural strength (MPa)	Fracture toughness ($MPa.m^{0.5}$)	Hardness (GPa)
D1	2.512 (0.239)	6.65 (0.96)	58.4 (6.8)	1.11 (0.17)	3.03 (0.24)
D2	2.564 (0.251)	6.48 (0.87)	62.2 (6.6)	1.16 (0.15)	3.05 (0.26)
D3	2.589 (0.267)	6.42 (0.95)	65.9 (5.9)	1.24 (0.10)	3.08 (0.19)
D4	2.521 (0.248)	6.74 (1.01)	57.2 (6.7)	1.15 (0.11)	3.04 (0.25)
D5	2.458 (0.225)	6.89 (1.05)	67.1 (7.8)	1.02 (0.08)	3.10 (0.30)
D6	2.486 (0.231)	6.39 (1.15)	73.3 (8.2)	1.03 (0.08)	3.12 (0.21)
D7	2.498 (0.245)	6.24 (0.94)	78.3 (7.4)	1.06 (0.13)	3.13 (0.27)
D8	2.487 (0.226)	6.97 (0.87)	64.6 (5.9)	1.01 (0.11)	3.12 (0.28)
D9	2.305 (0.218)	6.81 (1.02)	77.1 (7.4)	0.92 (0.09)	3.15 (0.24)
D10	2.317 (0.236)	6.68 (1.08)	82.1 (7.5)	0.94 (0.07)	3.16 (0.22)
D11	2.318 (0.033)	6.53 (1.34)	83.4 (8.3)	1.01 (0.10)	3.21 (0.19)
D12	2.304 (0.298)	6.84 (1.13)	74.6 (8.1)	0.96 (0.10)	3.15 (0.21)

* The estimated precision of these values is ± 3 %

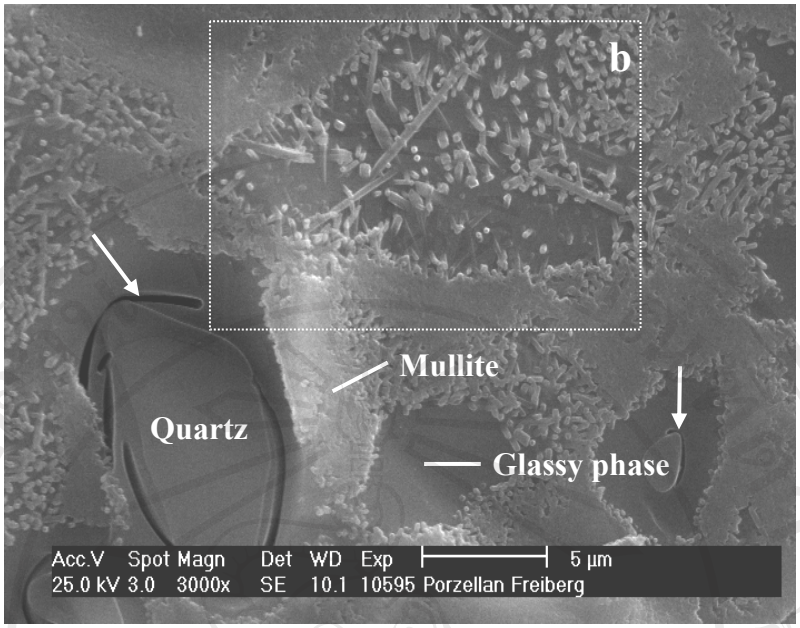

Fig. 4.1 SEM micrograph of dental porcelain ceramics.

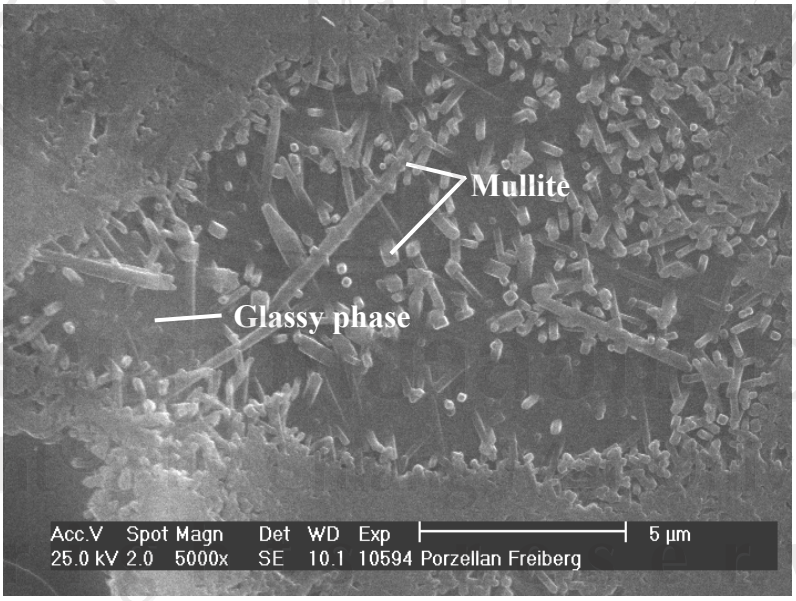

Fig. 4.2 Enlarge zone (b) demonstrating the formation of nanorod-mullite phase in the glassy matrix phase.

4.2 Al_2O_3 Reinforced Porcelain Ceramic Nanocomposites

Having prepared the dental porcelain ceramics (**D11**), the effect of Al_2O_3 on microstructural development and mechanical properties of the ceramics was investigated. In this section, test specimens were carefully examined with SEM technique to observe the microstructural developments (Figs. 4.3-4.6) and fracture paths (Figs. 4.7-4.8). Dental porcelain ceramics (**D11**) mainly showed the microstructure of a glassy matrix phase. All composite materials showed distinct two-phase structures with a glassy matrix phase and reinforcing alumina second phase, which was dispersed in the glassy matrix. Nanocrystalline Al_2O_3 clustering particularly at the edge of parent Al_2O_3 platelets were detected in **D13** (Fig. 4.3(a)). Recrystallization of Al_2O_3 clusters deposited on the surface of parent Al_2O_3 platelets was found in **D14** (Fig. 4.3(b)). Secondary recrystallized Al_2O_3 clusters (mean diameters ~ 0.5 μm) were found for **D15** (Fig. 4.4(a)) and ~ 50 nm - 0.5 μm for **D17** (Fig. 4.4(b)). Three different particle sizes (mean diameter ~ 100 nm - 10 μm) of microcrystalline Al_2O_3 phase, the same as the parent Al_2O_3-reinforced were detected in the **D18** (Fig. 4.5(a)) and **D19** ceramics (Fig. 4.5(b)). Microcrystalline Al_2O_3 phase (mean diameter ~ 0.4 μm) was found to disperse within the glassy phase of **D20** and **D21**. Part of the Al_2O_3-reinforcement phase agglomerated to a ball-like shape for **D20** (Fig. 4.6(a)) and a rounded sphere for **D21** (Fig. 4.6(b)).

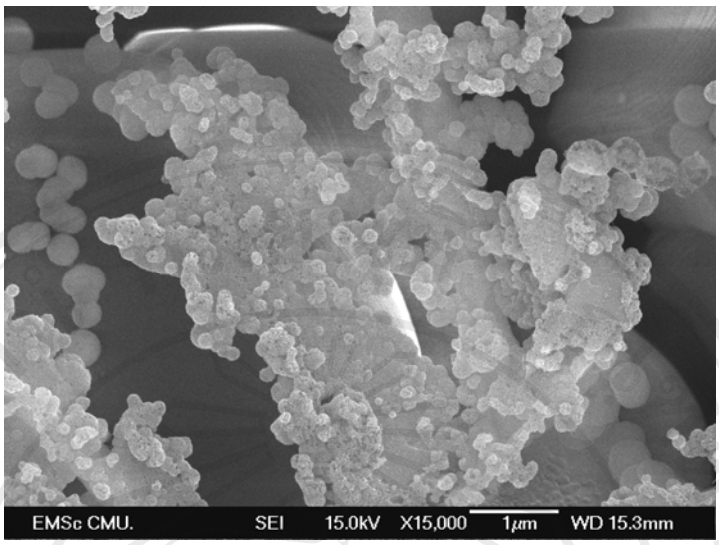

(a)

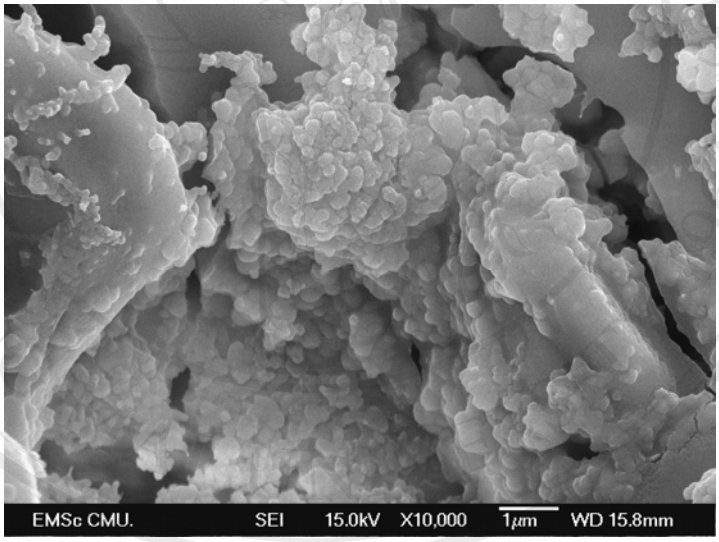

(b)

Fig. 4.3 SEM micrographs of Al_2O_3 (1-10 μm, platelet, α-phase) reinforced porcelain ceramics; (a) **D13** and (b) **D14**.

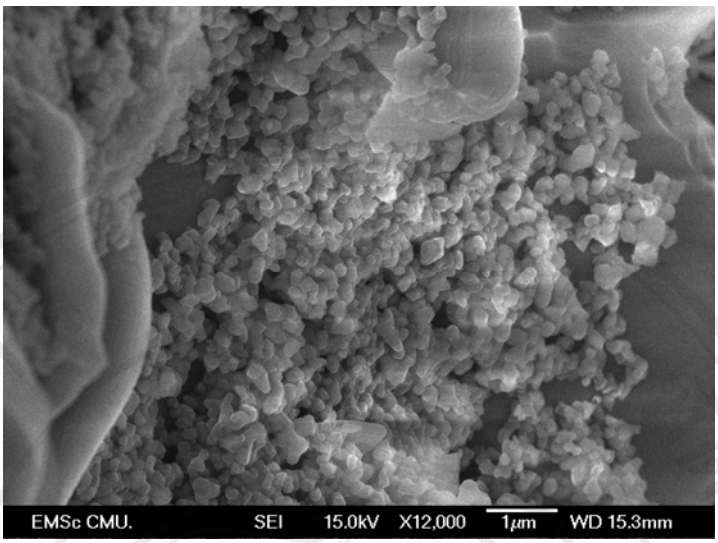

(a)

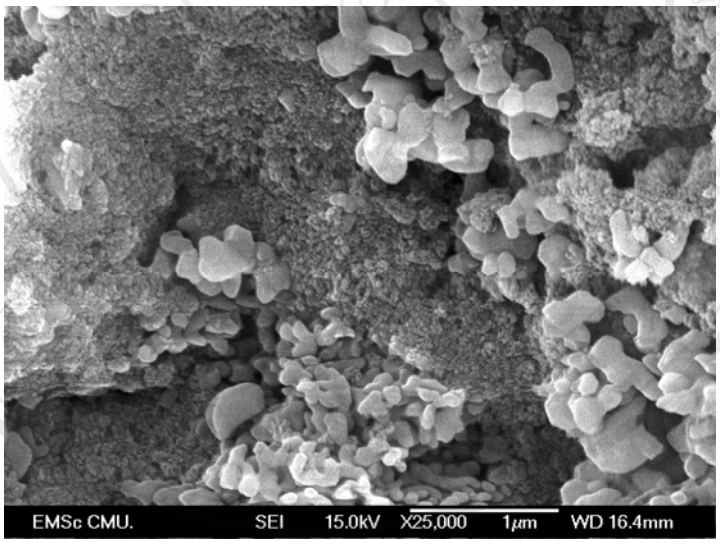

(b)

Fig. 4.4 SEM micrographs of Al_2O_3 (0.1-0.5 μm, irregular-shaped, α-phase) reinforced porcelain ceramics; (a) **D15** and (b) **D17**.

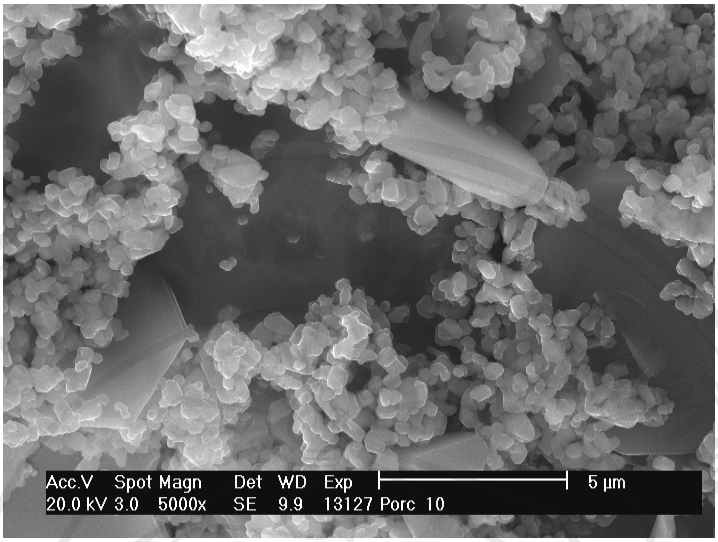

(a)

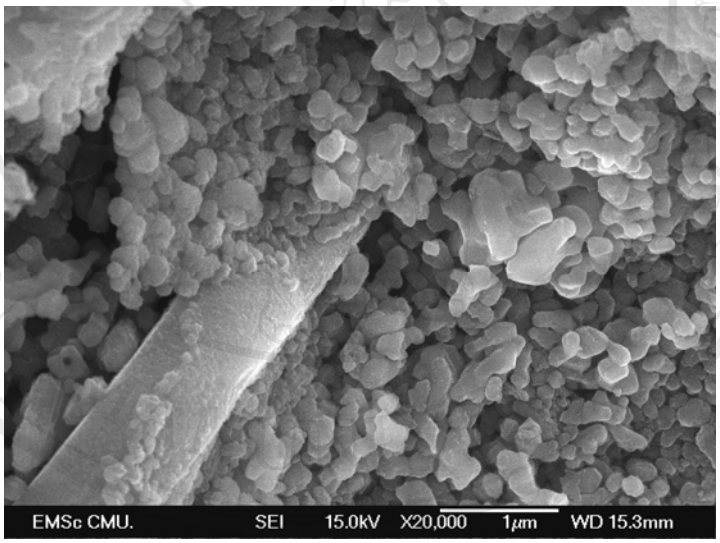

(b)

Fig. 4.5 SEM micrographs of Al_2O_3 (a mixture of 1-10 µm platelet, 0.1-1 µm irregular and 0.1-0.5 µm irregular; α-phase) reinforced porcelain ceramics; (a) **D18** and (b) **D19**.

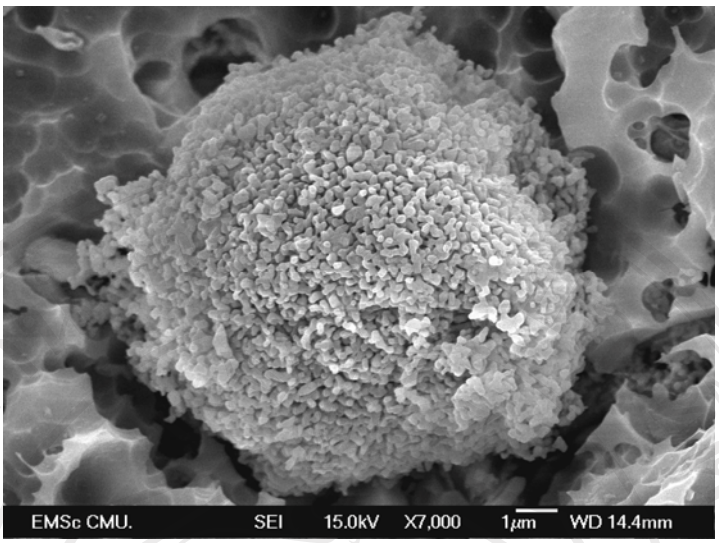

(a)

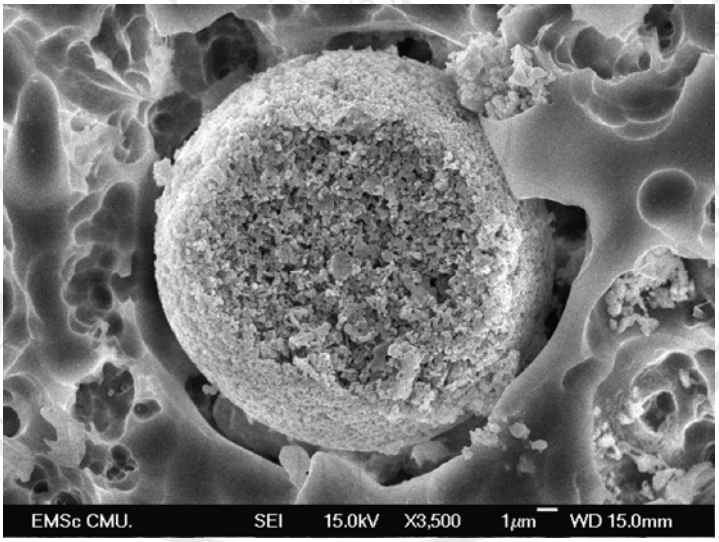

(b)

Fig. 4.6 SEM micrographs of Al_2O_3 (10-100 nm, fibrous-shaped, γ-phase) reinforced porcelain ceramics; (a) **D20** and (b) **D21**.

The cracks produced with the indenter are symmetric (Fig. 4.7). Cracks in the dental porcelain ceramics propagated directly through the glassy phase. For all Al_2O_3-reinforced porcelain ceramic specimens, the cracks mainly propagated intergranularly between alumina reinforced phases. Despite disparate evidence of several toughening mechanisms such as crack deflection, pullout of the grains with frictional interlock, bridging and microcracks, the crack patterns observed in these materials are similar (Fig. 4.8).

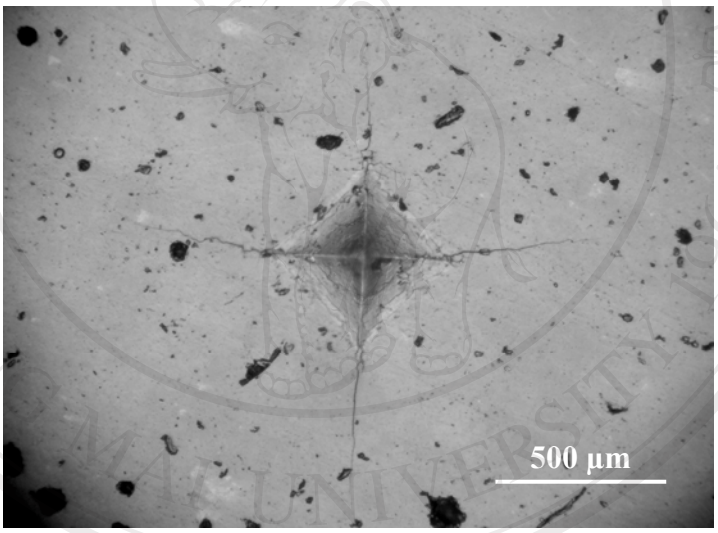

Fig. 4.7 Impression of a Vickers indenter producing symmetric cracks, where the cracks are propagating along the glassy phase of the matrix. The crack patterns are propagating normally to the orientation of the crystalline reinforced phase.

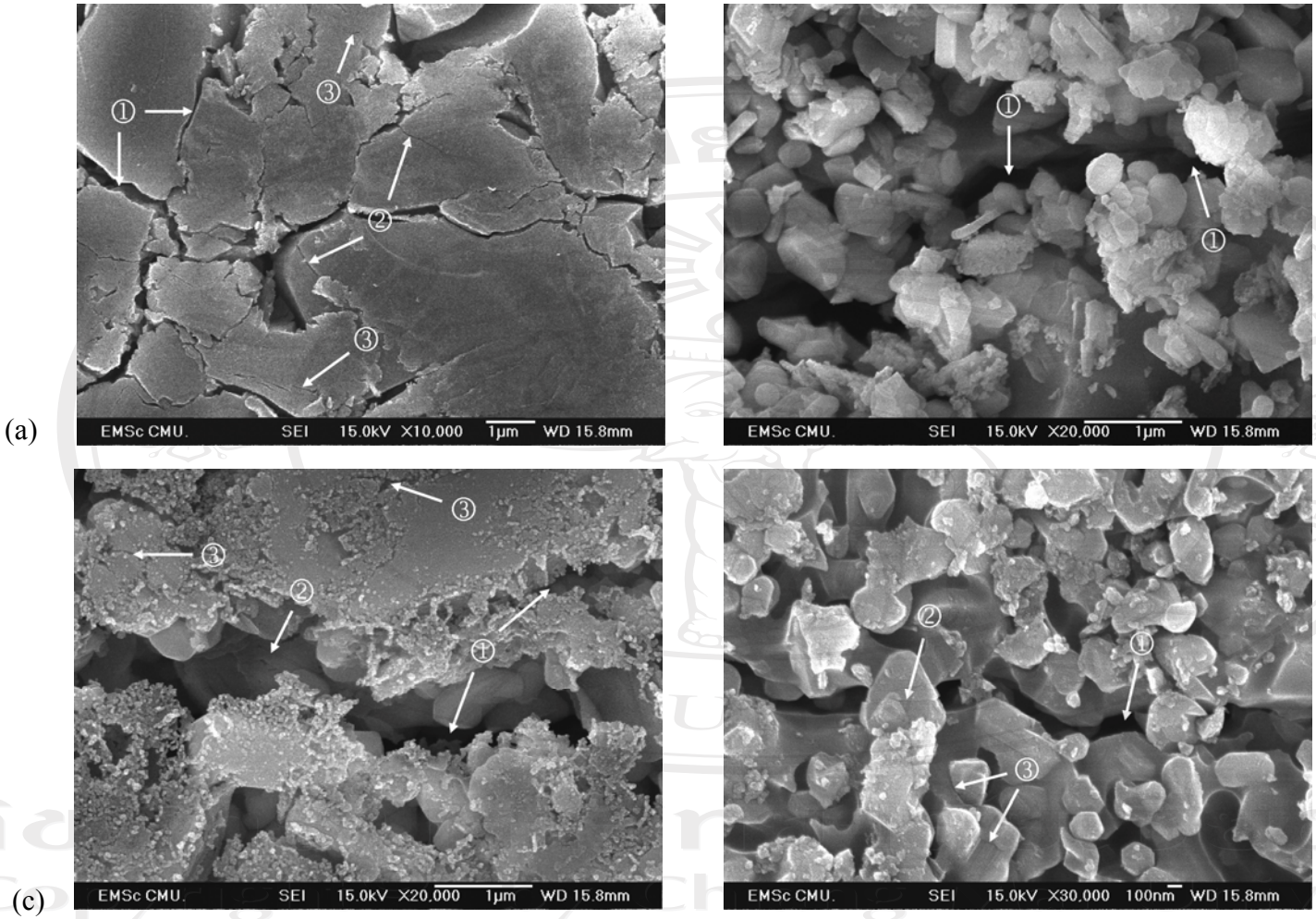

(a) (b) (c) (d)

Fig. 4.8 SEM micrographs of (a) **D14**, (b) **D17**, (c) **D19** and (d) **D21**; bridging ① a branch of the intergranular crack is propagating through a glassy phase, ② transgranular cracking through the grain of crystalline reinforced phase and ③ microcracks are visible in the glassy matrix and at the interface between particles and glass.

The sintering shrinkage and total porosity for all Al_2O_3-reinforced porcelain ceramics are presented in Table 4.2 and Fig. 4.19(a), uniaxial flexural strength and indentation fracture toughness are presented in Table 4.3 and Fig. 4.19(a), along with the corresponding standard deviation. Significant differences by one-way ANOVA and Scheffé post hoc test were calculated for porosity, strength and toughness data (Table 4.4). The results confirmed that the porosity values of almost all the samples were statistically similar to dental porcelain ceramics (**D11**) value ($p \geq 0.404$); only **D14**, **D16**, **D17** and **D21** have statistically significant higher porosity values ($p \leq 0.004$). **D17** (50 wt% of 0.1-0.5 μm, irregular-shaped, α-phase Al_2O_3) has the highest porosity in this group. The percentage shrinkage is correlated with the size of crystalline Al_2O_3 phase added and is highest in the group with Al_2O_3 (0.1-0.5 μm, irregular-shaped, α-phase) addition. All Al_2O_3-reinforced porcelain ceramic materials have statistically significant higher flexural strength values ($p < 0.001$) than pure dental porcelain. **D16** has the lowest strength and **D20** the highest strength of these materials. Although this value of **D20** is 10.9% greater than those of **D17** and **D21**, there is no statistically significant difference between them in the strength ($p \geq 0.059$).

Table 4.2 Average (and standard deviation) of the physical properties of Al_2O_3-reinforced porcelain ceramics.

Sample code	Shrinkage (%)	Bulk density (g/cm^3)	Total porosity (%)
D11	15.75 (0.50)	2.318 (0.033)	6.53 (1.34)^{a,b,c}
D13	16.11 (0.47)	2.614 (0.035)	7.54 (1.28)^{b,c,d}
D14	11.80 (0.61)	2.508 (0.032)	9.25 (1.19)^{d,e}
D15	20.40 (0.58)	2.527 (0.024)	5.30 (0.91)^{a}
D16	23.74 (0.54)	2.498 (0.033)	10.16 (1.20)^{e}
D17	22.04 (0.54)	2.421 (0.037)	13.21 (1.35)^{f}
D18	15.79 (0.43)	2.525 (0.024)	5.84 (0.91)^{a,b}
D19	15.64 (0.25)	2.591 (0.025)	7.55 (0.89)^{b,c,d}
D20	18.18 (0.43)	2.497 (0.033)	8.16 (1.22)^{c,d,e}
D21	18.44 (0.43)	2.457 (0.037)	9.30 (1.36)^{d,e}

[a-e] There is no significant statistical different ($p > 0.05$) between materials with the same superscript letters.

Table 4.3 Average (and standard deviation) of the mechanical properties of Al_2O_3-reinforced porcelain ceramics.

Sample code	Flexural strength (MPa)	Coefficient of strength variation (%)	Fracture toughness ($MPa \cdot m^{1/2}$)	Elastic modulus (GPa)	Hardness (GPa)
D11	83.4 (8.3)[a]	9.9	1.01 (0.10)[a]	58.8 (6.6)	3.21 (0.19)
D13	133.3 (11.8)[b,c,d]	8.8	1.73 (0.17)[b,c]	119.2 (13.4)	6.24 (0.50)
D14	124.0 (14.2)[b,c]	11.4	1.44 (0.14)[b]	84.8 (7.2)	4.65 (0.10)
D15	119.6 (20.0)[b]	16.7	1.39 (0.13)[b]	79.6 (6.8)	4.35 (0.10)
D16	119.1 (22.6)[b]	18.9	1.43 (0.15)[b]	81.0 (8.0)	4.41 (0.10)
D17	148.7 (13.5)[d,e]	9.0	1.92 (0.21)[c]	134.4 (16.6)	7.21 (0.47)
D18	135.4 (17.7)[b,c,d]	13.0	1.69 (0.19)[b,c]	112.4 (12.8)	6.07 (0.39)
D19	132.7 (19.1)[b,c,d]	14.3	1.61 (0.23)[b,c]	104.0 (18.0)	5.46 (0.58)
D20	165.0 (18.0)[e]	10.9	2.31 (0.24)[d]	170.4 (18.0)	8.23 (0.56)
D21	143.2 (17.5)[c,d,e]	12.2	1.84 (0.20)[c]	127.0 (13.4)	6.65 (0.18)

[a-d] There is no significant statistical different ($p > 0.05$) between materials with the same superscript letters.

Table 4.4 Summary of one-way ANOVA of Al_2O_3-reinforced porcelain ceramics.

Total porosity (%)

Source	**SS**	***df***	**MS**	**F**	**Sig.**
Material	488.061	9	54.229	38.697	< 0.001
Residual	126.124	90	1.410		

Uniaxial flexural strength (MPa)

Source	**SS**	***df***	**MS**	**F**	**Sig.**
Material	84574.009	9	9397.112	33.208	< 0.001
Residual	53765.381	190	282.976		

Indentation fracture toughness ($MPa \cdot m^{1/2}$)

Source	**SS**	***df***	**MS**	**F**	**Sig.**
Material	11.198	9	1.244	36.124	< 0.001
Residual	3.100	90	0.034		

SS: Sum Squares; ***df***: Degrees of freedom; **MS**: Mean Squares; **F**: MS of material/MS of residual; **Sig.**: significance.

The flexural strength results of the Weibull analysis are presented in Table 4.5, together with the Weibull plots (Figs. 4.9 and 4.10). High Weibull moduli (steeper lines) indicated more uniform strength. Only **D11**, **D13**, **D18** and **D19** showed good correlations with the regression used, according to the values of the 90% critical correlation coefficient (r). The statistical significance between the strength of materials tends towards that obtained by one-way ANOVA, where data sets were compared for the overlap of their double-sided confidence intervals at the 95% level. The high Weibull modulus for **D11**, **D13**, **D14**, **D17** and **D20** indicated a uniform material with reliable strength values. On the other hand, **D15** and **D16** had wider ranges of strength values with lower Weibull moduli. The toughness of the dental porcelain lies within the same range as observed by Craig and Powers [21]. Consistency with their reported data indicated the reliability of the indentation technique in evaluating the toughness of specimens. The results also confirmed that all the Al_2O_3-reinforced porcelain ceramics evaluated in this study are statistically significantly tougher ($p < 0.001$) than pure dental porcelain ceramics (**D11**). As with the flexural strength results, **D20** is the toughest ($p < 0.001$) of all the ceramics; **D13**, **D17**, **D18**, **D19** and **D21** showed medium toughness with no statistically significant difference ($p \geq 0.143$) between them, while the others had the lowest toughness.

Table 4.5 Results of the Weibull regression analysis of Al_2O_3-reinforced porcelain ceramics.

Sample code	*m* Value	σ 0.01 (MPa)	σ 0.05 (MPa)	σ 0.10 (MPa)	r^2	σ_0	C.I. (95%) for σ_0
D11	11.84	58.8	67.4	71.7	0.9712	86.7[a]	82.8 - 90.6
D13	13.45	98.3	111.0	117.1	0.9588	138.5[b,c]	132.9 - 144.0
D14	10.32	84.1	98.5	105.6	0.8881	131.4[b]	124.7 - 138.0
D15	7.18	68.8	86.4	95.5	0.8476	130.6[b]	121.2 - 140.0
D16	6.01	59.7	78.4	88.3	0.8348	128.5[b]	117.9 - 139.1
D17	12.48	107.3	122.3	129.6	0.8226	155.2[d]	148.9 - 161.6
D18	8.49	82.2	99.6	108.4	0.9473	141.3[b,c]	133.0 - 149.6
D19	7.99	78.5	96.3	105.4	0.9722	139.7[b,c]	130.8 - 148.7
D20	10.21	109.6	128.6	138.0	0.8444	172.0[e]	163.6 - 180.5
D21	9.39	92.0	109.5	118.2	0.8932	150.2[c,d]	142.0 - 158.4

[a-e] There is no significant Weibull statistical different ($p > 0.05$) between materials with the same superscript letters. *m* value is the Weibull modulus; σ 0.01, 0.05 and 0.10 is the stress levels at 1, 5 and 10% probability of failure, respectively; r^2 is the regression coefficient; σ_0 is the Weibull characteristic strength; C.I. is the confidence intervals.

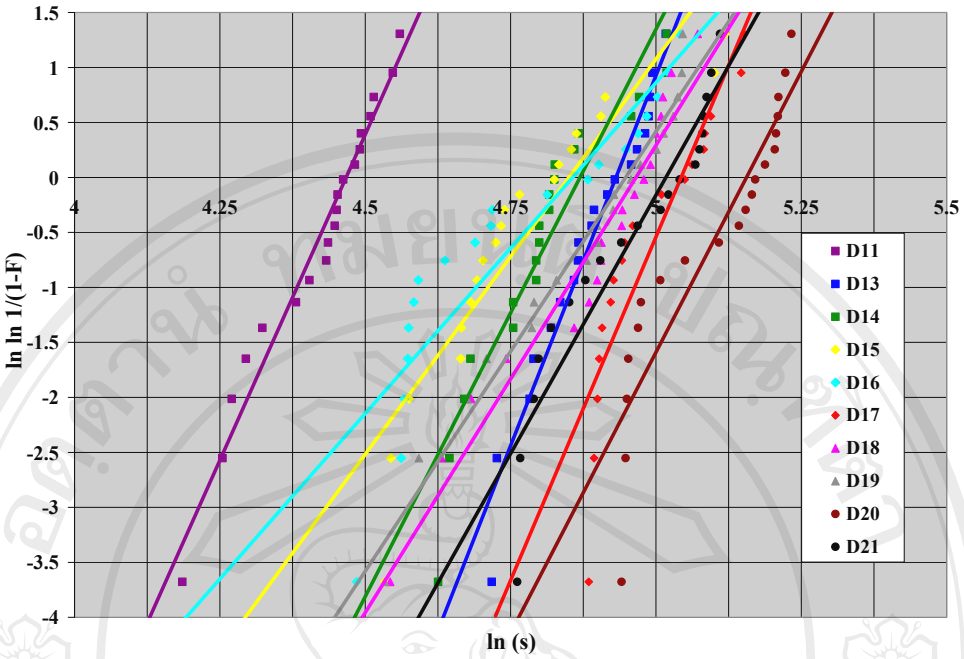

Fig. 4.9 Weibull plots of uniaxial flexure strength data for Al_2O_3-reinforced porcelain ceramics.

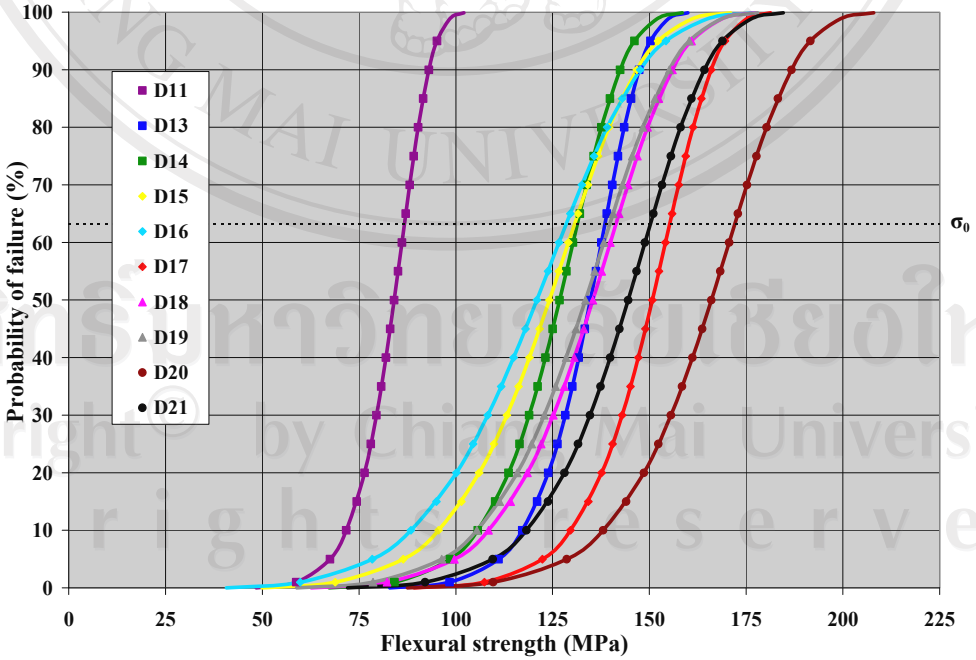

Fig. 4.10 The cumulative Weibull plots of probability of failure data for Al_2O_3-reinforced porcelain ceramics.

The mechanical properties of glass matrix composites are affected, in addition to crystallization of glass, by the reinforcement. The flexural strength of Al_2O_3-reinforced porcelain ceramics was found to statistically significant increase compared with pure dental porcelain (**D11**), enhancing up to 42.8 - 97.8%. This result has a good agreement with the literature [139,140]. Types of reinforced materials were also affected to the strength of composite materials in the same amount of additive. The reinforcement with Al_2O_3 (10-100 nm, fibrous-shaped, γ-phase) tended to create higher strength than the others. This effect is caused by recrystallization of alumina from the nanosize alumina phase added and its good homogeneous dispersion in the matrix phase after sintering. This is also due to the higher sintering activity of nanopowders [141,142]. The sintering shrinkage has correspondence with the size of crystalline Al_2O_3 phase added. The effect is found that, the particle size of nanocrystalline or fibrous-shaped alumina (10-100 nm), strongly affects the statistically significant difference in this property. This is probably caused by the higher compaction degree in shaping of the materials [143]. Another one likely secondary effect is found that in composite materials which obtained a high heating rate and short time sintering entrapment of gas inside occurs. The sintering starts at the surface and the pores were closed. Nanocrystalline additives were found to be not suitable for this process.

In the case of the same type reinforcing materials, the strength of almost all composites were found to be not statistical significant relatively with the amount of additives. This is caused by the influence of reinforcement content on the mechanical resistance of glass matrix composites may become more evident when high porosity and low density occurs. Even if glass matrix composites were rarely characterized by

higher densification, these composites showed higher bending strength. The same as flexural strength, Vickers hardness of glass matrix composites showed a certain dependence on residual porosity.

As expected, hardness in Al_2O_3-reinforced porcelain ceramics increases with increasing alumina content (alumina is much harder than glass), but the enhancement was reduced by the effect of porosity. The values of porosity varied from 9.25 to 13.21%, being higher than in the dental porcelain (6.53%), especially for the highest content of reinforced materials (**D14**, **D17**, **D19**, and **D21**). The presence of rigid clusters cause the densification to be retarded and the effective viscosity of the materials are much higher than that the matrix alone. The reinforcement decreases the viscous flow ability of dental porcelain deeply depending on its aspect ratio [10]. In order to balance the retardation during sintering caused by the reinforcements, the sintering temperatures for glass matrix composites were 180 °C higher than that of un-reinforced matrix [144]. Higher reinforcement volume fraction or higher aspect ratios would lead to the higher porosity. This is consistent with the assumption of a decreasing viscous flow ability of dental porcelain with increasing concentration of inclusions [145,146]. The fact that for every higher concentration, the porosity content is almost constant suggests that the sintering ability is influenced not only by the amount of non-sintering inclusions but also by secondary effects, which are dependent from the morphology of inclusions and also depend on the sintering process [147,148]. Samples with high content of Al_2O_3 additives showed a trend of slight strength decrease, while samples with low content of alumina which have higher densification (lower porosity) showed the highest values.

The fracture toughness of Al_2O_3-reinforced porcelain ceramics was found to statistically significant increase up to 37.6 - 128.7% compared with pure dental porcelain ceramics. Fracture toughness (K_{IC}) exhibited a decreasing trend with increasing alumina content, but within the same content or same type of reinforcing materials no significant statistical different in this values occurred. The higher toughness of nine composite materials compared to dental porcelain may be the result of the reinforcing second phase. Higher fracture toughness occurs more often in two-phase materials than in single-phase materials if the second reinforced phase makes crack propagation more difficult, due to the formation of the crack requires higher energy [149]. A crack deflection toughening was found to be effective; this causes the fracture surfaces to be extremely rough in relation to that of parent ceramic. Cracks deviate around the reinforcement, as illustrated in the fracture surfaces in Fig. 4.8, in good agreement with the findings in the literature [11,150]. The presence of rigid clusters, alumina reinforcing phase and especially nanocomposite structure formations, probably made crack propagation more difficult and contributed to the high toughness of these materials.

The SEM micrographs showed a good dispersion of reinforcement caused by vibro-milling technique. Not surprisingly, dental porcelain ceramic having a much greater content of glass and lower content of reinforcing material, it is the weakest ceramic of this studied (Tables 4.3 and 4.4). The microscope observations reported in this study support previous statement regarding the bending strength and toughening mechanism [84], which is based on a uniform distribution of the alumina crystals and the microcrack toughening due to the mismatch of the coefficient of thermal expansion between the crystalline and glassy phases (Fig. 4.8(a,c,d)). The role of the

microcracks in glass-ceramics system is contradictory discussed [151,152]. It has been proposed that the microcracks can contribute crack deflection and dispersing its energy [153]. This effect increases the strength and fracture toughness of a given ceramic. However, if cluster of crystals are present, microcracks tend to coalesce, forming a crack, which surrounds the cluster (decoupling of alumina particles) as if it were a single grain and thus causing a degeneration of the strength and fracture toughness [11]. Low magnification micrographs taken from etched specimens showed the presence of bands where clusters of crystals appeared denser, apparently aligned and affecting the crack propagation. On the other hand, observations at higher magnification are not always consistent, showing areas with apparent preferred alignment of the crystals along with other regions where the grains are randomly distributed (Fig. 4.8). The toughening was a possible mechanism in fine grain size ceramic (< 20 μm [154]); it may hence be a possible mechanism in nanocrystalline or fibrous-shaped alumina reinforced materials. The nanocrystalline phase formations with some aspect ratio are thought to be the reason of the relevant increase in bending strength, hardness and fracture toughness, despite residual porosity typical of fast firing and one step sintering treatment. However, observation of their contribution to the ultimate fracture toughness requires an approach somewhat more complicated than used in the present study.

The presence of large particle inclusions or particle agglomerates with critical size has been associated with extensive microcracking in the glassy matrix [155]. The produced stress raises higher than that from the inherent flaws as the energy for the flaw to grow is potentially provided by the elastic stored energy in the particle and the adjacent glassy matrix. The introduction of small rather than larger particle into a

glassy matrix has produced minimal microcracking and flexural strength improvements in different composite systems [132,156]. The Weibull distributions are narrower for example **D20** and **D17** as would be expected as surface roughness, flaw size and distribution have been shown to effect the Weibull distribution of strength values.

This study showed that in general an increase of crystalline content of Al_2O_3-reinforced in dental porcelain is accompanied with an increase of the strength and fracture toughness of reinforced materials. However, in materials with comparable crystalline content, some other factors such as porosity, grain size, shape and orientation are important in determining the physical and mechanical properties [157,158]. All Al_2O_3-reinforced porcelain ceramics recorded higher strengths and toughness value than standard dental porcelain. The difference in type of crystalline Al_2O_3 phase, especially the crystalline size or shaped of Al_2O_3 additives, have more influence on the mechanical properties. At the same condition, the minimal variations of the grain size, shape and orientation, especially in the nanocomposite structures, strongly affects the strength and toughness of materials also. The Weibull moduli indicated that almost all of composite materials had a good strength characteristic.

Apart from the Al_2O_3 additive, the effect of a combination between Al_2O_3 and other crystalline phases such as TiO_2, MgO and ZnO was also investigated as detail given in the next section.

4.3 Al_2O_3-M_xO_y Reinforced Porcelain Ceramic Nanocomposites

In analogous to the previous section, here attention is given to the phase formation, microstructure, densification and mechanical properties of Al_2O_3-M_xO_y reinforced porcelain ceramic system. Significant data obtained from the XRD analyses of all materials are given in Tables 4.6 and 4.7. The analyses showed the diffraction pattern (Figs. 4.11 and 4.12) after firing of composite material powders which are compared with dental porcelain (Fig. 4.11). The dental porcelain (**D11**) analysis shows the presence of the peaks corresponding to mainly tetragonal leucite phase. The dominant peaks of **D22** - **D25** are rhombohedral alumina phase. The dominant peaks of cubic gahnite ($ZnAl_2O_4$), the new phase formation, were found in **D26** and **D27**. Cubic spinel ($MgAl_2O_4$) was also found in **D24**.

Table 4.6 XRD analysis of Al_2O_3 - M_xO_y reinforced porcelain ceramics.

Sample code	Detected crystalline phases			
	Al_2O_3	$KAlSi_2O_6$	$MgAl_2O_4$	$ZnAl_2O_4$
D11	✓	✓		
D22	✓			
D23	✓			
D24	✓		✓	
D25	✓			✓
D26	✓			✓
D27	✓			✓

Table 4.7 Detected crystalline phase specification.

Crystalline phase (chemical formula)	**PDF number**	**Crystal system**	**References**
Leucite ($KAlSi_2O_6$)	15-0047	Tetragonal	[159,160]
Corundum/Alumina (Al_2O_3)	10-0173	Rhombohedral	[161,162]
Spinel ($MgAl_2O_4$)	21-1152	Cubic	[163,164]
Gahnite ($ZnAl_2O_4$)	05-0669	Cubic	[165,166]

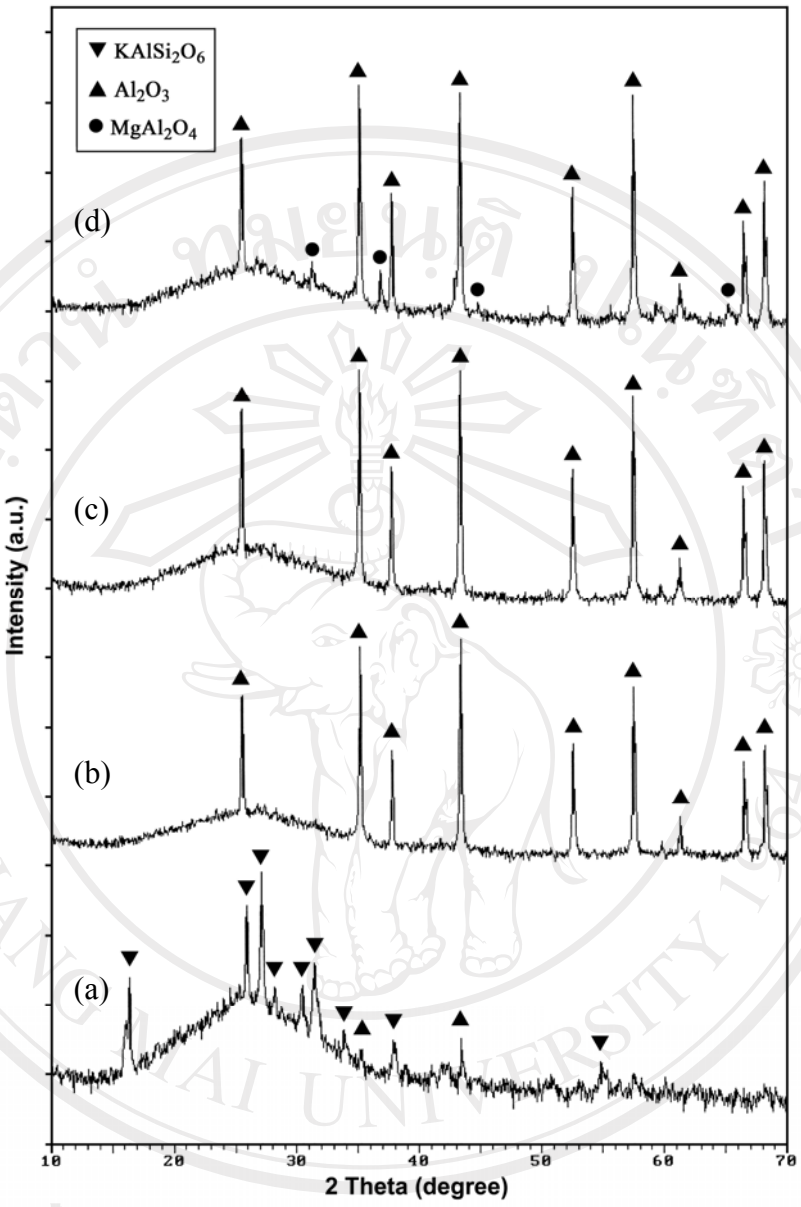

Fig. 4.11 X-ray diffraction patterns of (a) pure dental porcelain ceramic (**D11**) and Al_2O_3-M_xO_y reinforced porcelain ceramics; (b) **D22**, (c) **D23** and (d) **D24**.

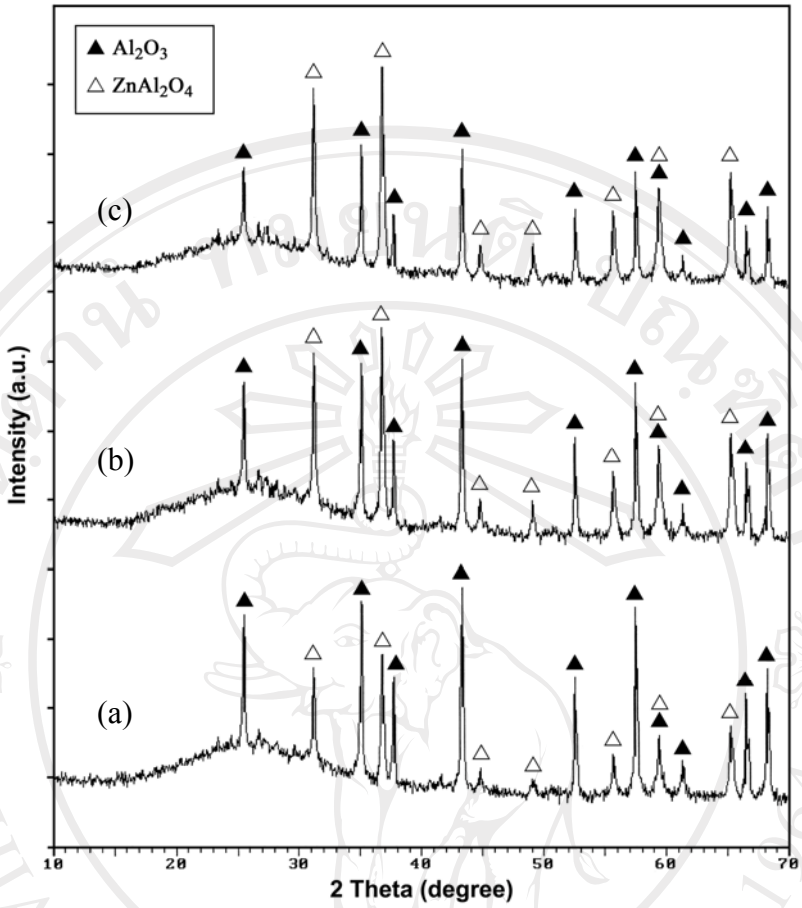

Fig. 4.12 X-ray diffraction patterns of Al_2O_3-M_xO_y reinforced porcelain ceramics; (a) **D25**, (b) **D26** and (c) **D27**.

The observation of microstructure, nanocomposite material formations and fracture paths for each composite material were examined by the SEM. All materials showed the distinct two (or more) phase structures with a glassy matrix phase and reinforcing crystalline phase, which is dispersed in a glassy matrix. The **D22** ceramic (Fig. 4.13(a)) showed the formation of nanocomposite structure as a needle-like (~ 50 nm in diameter and 1 μm in length) at the edge of parent alumina grains. The **D23** ceramic (Fig. 4.13(b)) has a fine microstructure (mean diameter ~ 0.5 - 1 μm) with the agglomerates. The **D24** ceramic (Fig. 4.13(c)) is observable in three forms: large faceted grains, fine spherical (mean diameter ~ 0.2 - 0.4 μm) and platelet grains (~ 1x1x0.5 μm). The **D25** ceramic (Fig. 4.14(a)) showed a fine microstructure with the agglomerates as **D23**. For **D26** (Fig. 4.14(b)) and **D27** ceramics (Fig. 4.14(c)), the additives are observable in two forms: the agglomerates as found in **D25** and the nanocomposite materials formation of the reticulate sheets (100 nm thickness).

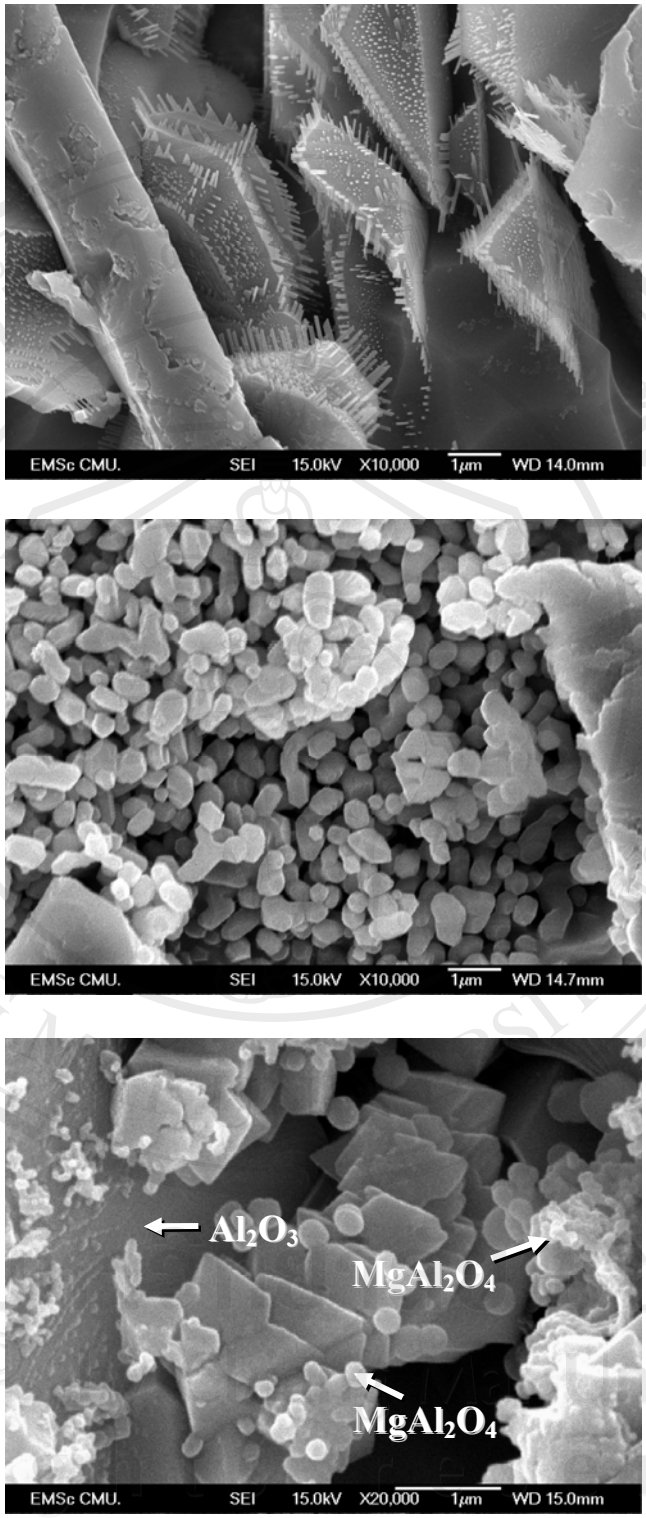

Fig. 4.13 SEM micrographs of Al_2O_3 - M_xO_y (TiO_2, MgO) reinforced porcelain ceramics; (a) **D22**, (b) **D23** and (c) **D24**.

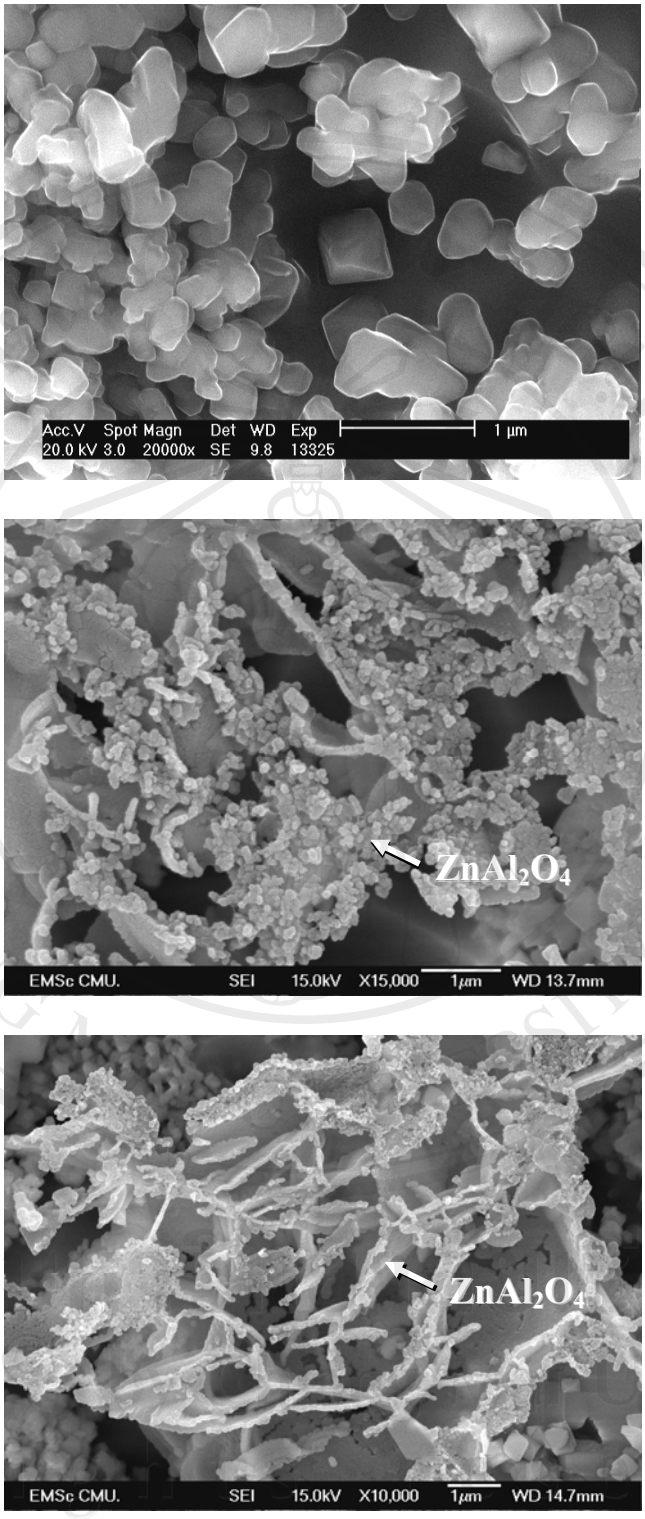

Fig. 4.14 SEM micrographs of Al_2O_3 (10-100 nm, fibrous-shaped, γ-phase) - ZnO reinforced porcelain ceramics; (a) **D25**, (b) **D26** and (c) **D27**.

Indentations of all Al_2O_3 - M_xO_y reinforced porcelain ceramics show asymmetric cracks (Fig. 4.15). The crack pattern is consistently transgranular for Al_2O_3 grains, where as it is mainly intergranular for alumina grains, excepted when the crack tip propagates perpendicularly to the transverse grains (Fig. 4.16(a,b)). SEM micrograph shows evidence of crack deflection and crack shielding (bridging and pull-out of reinforcing grains) (Fig. 4.16) and microcrack toughening (Fig. 4.16(b-d)).

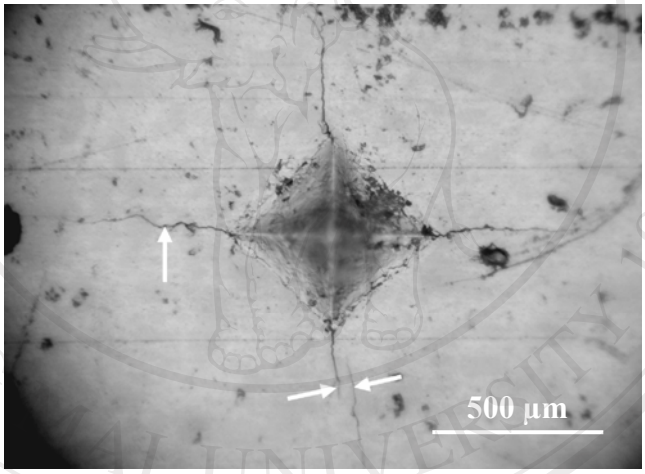

Fig. 4.15 Optical micrograph of asymmetric cracks from the corners of an indentation of composite materials in this section with propagating of cracks along the glassy matrix phase and retarded (non-directly line) with the crystalline reinforced phase (arrows).

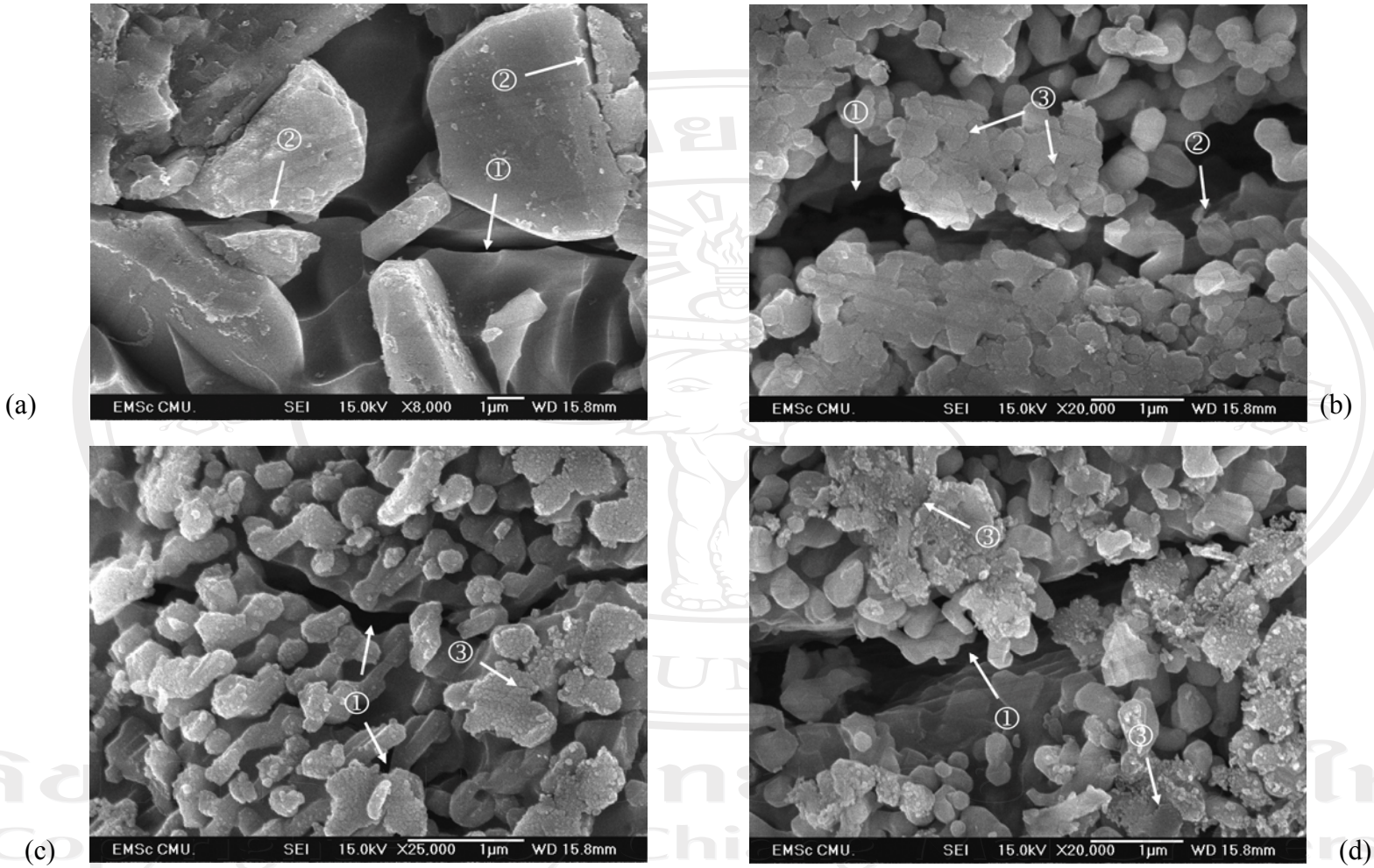

Fig. 4.16 SEM micrographs of (a) **D22**, (b) **D23**, (c) **D24** and (d) **D27**; bridging ① a branch of the intergranular crack is propagating through a glassy phase, ② transgranular cracking through the grain of crystalline reinforced phase and ③ microcracks are visible in the glassy matrix and at the interface between particles and glass.

The sintering shrinkage and total porosity for all Al_2O_3 - M_xO_y reinforced porcelain ceramics are presented in Table 4.8 and Fig. 4.19(b), uniaxial flexural strength and indentation fracture toughness are presented in Table 4.9 and Fig. 4.19(b), along with the corresponding standard deviation. Significant differences by one-way ANOVA analysis and Scheffé post hoc test were calculated for the porosity, strength and toughness data (Table 4.10). The results confirmed that the porosity values of almost all these composites were statistically similar to dental porcelain (**D11**) value ($p > 0.20$), only **D22** has statistically significant higher porosity value ($p < 0.001$). The sintering shrinkage of all composite materials was slightly greater than that of pure dental porcelain (the weakest materials). All materials have statistically significant greater flexural strength values ($p < 0.001$) than the un-reinforced dental porcelain. **D22** has the lowest strength and **D23** the highest of these materials. Although the flexural strength value of **D27** is greater than those of **D26** and **D25**, there is no significant statistical different ($p \geq 0.257$) in these materials.

Table 4.8 Average (and standard deviation) of the physical properties of Al_2O_3-M_xO_y reinforced porcelain ceramics.

Sample code	Shrinkage (%)	Bulk density (g/cm^3)	Total porosity (%)
D11	15.75 (0.50)	2.318 (0.033)	6.53 (1.34)^{a,b}
D22	16.98 (0.79)	2.422 (0.037)	11.40 (1.35)^{c}
D23	19.52 (0.32)	2.643 (0.044)	7.02 (1.55)^{a,b}
D24	17.56 (0.65)	2.657 (0.023)	6.03 (0.83)^{a}
D25	18.36 (0.61)	2.620 (0.030)	6.96 (1.10)^{a,b}
D26	18.94 (0.29)	2.656 (0.023)	7.02 (0.82)^{a,b}
D27	18.04 (0.39)	2.644 (0.024)	8.07 (0.84)^{b}

^{a,b} There is no significant statistical different ($p > 0.05$) between materials with the same superscript letters.

Table 4.9 Average (and standard deviation) of the mechanical properties of Al_2O_3-M_xO_y reinforced porcelain ceramics.

Sample code	Flexural strength (MPa)	Coefficient of strength variation (%)	Fracture toughness ($MPa \cdot m^{1/2}$)	Elastic modulus (GPa)	Hardness (GPa)
D11	83.4 (8.3)[a]	9.9	1.01 (0.10)[a]	58.8 (6.6)	3.21 (0.19)
D22	125.1 (19.9)[b]	15.9	1.62 (0.18)[b]	112.8 (11.0)	6.02 (0.38)
D23	201.3 (21.9)[c]	10.8	2.61 (0.25)[c]	185.4 (16.2)	8.60 (0.74)
D24	125.7 (19.6)[b]	15.5	1.63 (0.19)[b]	110.2 (15.0)	5.56 (0.43)
D25	135.5 (24.7)[b,d]	18.2	1.83 (0.22)[b,d]	135.2 (14.6)	6.96 (0.13)
D26	146.3 (14.8)[b,d]	10.1	2.00 (0.20)[d]	147.0 (14.4)	7.44 (0.47)
D27	152.4 (19.8)[d]	12.9	2.04 (0.23)[d]	150.4 (19.0)	7.17 (1.03)

[a-d] There is no significant statistical different ($p > 0.05$) between materials with the same superscript letters.

Table 4.10 Summary of one-way ANOVA of Al_2O_3-M_xO_y reinforced porcelain ceramics.

Total porosity (%)

Source	**SS**	***df***	**MS**	**F**	**Sig.**
Material	193.609	6	32.268	24.092	< 0.001
Residual	84.382	63	1.339		

Uniaxial flexural strength (MPa)

Source	**SS**	***df***	**MS**	**F**	**Sig.**
Material	151644.93	6	25274.155	68.891	< 0.001
Residual	48793.74	133	366.870		

Indentation fracture toughness ($MPa \cdot m^{1/2}$)

Source	**SS**	***df***	**MS**	**F**	**Sig.**
Material	14.480	6	2.413	57.218	< 0.001
Residual	2.657	63	0.042		

SS: Sum Squares; ***df***: Degrees of freedom; **MS**: Mean Squares; **F**: MS of material / MS of residual; **Sig.**: significance.

The results of the Weibull analyses for the flexural strength are presented in Table 4.11, together with the Weibull plots (Figs. 4.17 and 4.18). High Weibull moduli (steeper lines) indicated more uniform strength. All tested materials had good fits to the regression used, excepted for **D23** and **D26**, according to the difference between the coefficients of determination (r^2) values. The statistical significance between the strength of materials had trended to the same as which analyzed by one-way ANOVA, when data sets were compared for the overlap of their double sided confidence intervals at the 95% level. The high Weibull modulus only for dental porcelain (**D11**), **D23** and **D26** indicated a uniform material with reliability of the strength. The results also confirmed that all materials evaluated in this study have statistically significant tougher ($p < 0.001$) than the dental porcelain. The same as flexural strength results, **D23** is also the toughest ($p < 0.001$), **group 11** (**D25** - **D27**) had an intermediate and no significant statistical different ($p \geq 0.529$) between them, the others had the lowest.

Table 4.11 Results of the Weibull regression analysis of Al_2O_3-M_xO_y reinforced porcelain ceramics.

Sample code	*m* Value	σ 0.01 (MPa)	σ 0.05 (MPa)	σ 0.10 (MPa)	r^2	σ_0	C.I. (95%) for σ_0
D11	11.84	58.8	67.4	71.7	0.9712	86.7[a]	82.8 - 90.6
D22	6.96	68.1	86.0	95.4	0.9487	131.9[b]	122.6 - 141.2
D23	10.67	137.1	159.8	170.9	0.8842	211.1[c]	200.8 - 221.4
D24	6.81	67.1	85.3	94.8	0.9270	131.9[b]	122.7 - 141.1
D25	6.16	68.5	89.3	100.3	0.9101	144.6[b,d]	133.0 - 156.2
D26	11.68	103.7	119.3	126.9	0.8929	153.8[d,e]	146.9 - 160.8
D27	8.93	95.7	114.9	124.5	0.9682	160.2[e]	151.0 - 169.5

[a-e] There is no significant Weibull statistical different ($p > 0.05$) between materials with the same superscript letters. Details of the values were as described in Table 4.5.

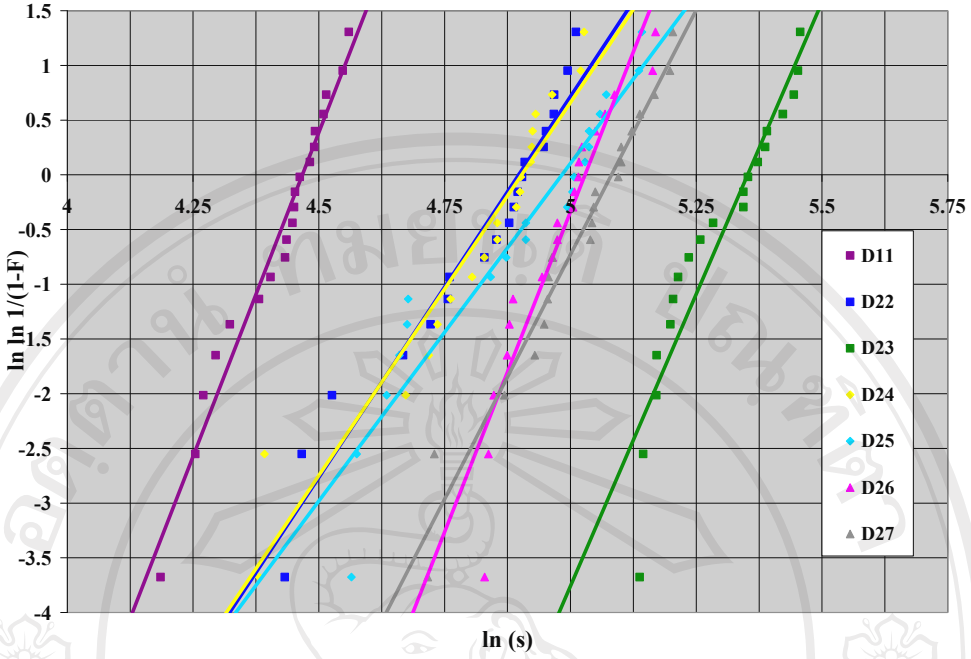

Fig. 4.17 Weibull plots of flexure strength data for Al_2O_3-M_xO_y reinforced porcelain ceramics.

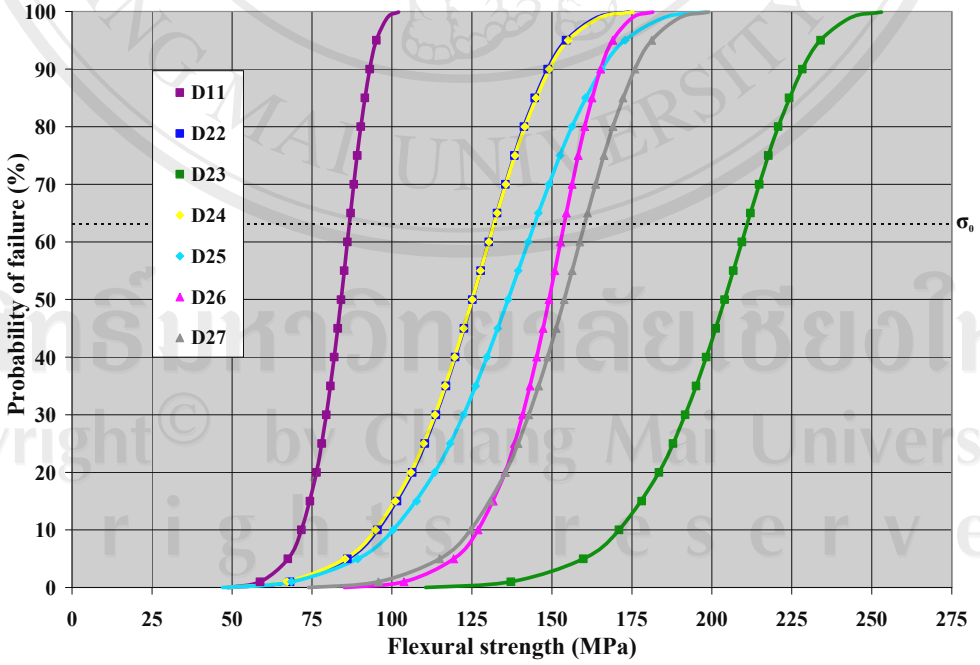

Fig. 4.18 The cumulative Weibull plots of probability of failure data for Al_2O_3-M_xO_y reinforced porcelain ceramics.

Although the color results were not showed, the color of all Al_2O_3-M_xO_y reinforced porcelain ceramics found not much different from the dental porcelain, they are within the same range of white color as described by ISO 6872 [122]. The mechanical properties of glass matrix composites are affected, in addition to crystallization of glass, by the reinforcement as reported in topic 4.1. The flexural strength of all composites was found significant statistical different compared with pure dental porcelain (**D11**), increasing up to 50 - 141.3% (Table 4.9). In this study, the porosity is effected by the presence of added rigid additive. The densification is retarded and the effective viscosity of the composite materials is much higher than that the matrix alone. The additive will decrease the viscous flow ability of dental porcelain, but all of them had no significant difference compared with dental porcelain. Only the **D22** had difference, caused by the difference in grain size among the additives and the ceramic matrix. This effect is also caused by the higher sintering temperatures and time for glass matrix composites, to balance the retardation during sintering. However, the deviation from the complete densification of the sintered materials was attributed to the porosity. The pore value could be considered detrimental to the mechanical properties. Despite the non significant residual porosity observed, the bending strength of the sintered composite materials was notable.

In the case of different types of alumina additives, **D22** and **D23**, the Al_2O_3 (10-100 nm, fibrous-shaped, γ-phase) was found to be suitable for the reinforcement of dental porcelain. The achieved bending strength was attributed to the formation of strong bond between the glass matrix and the reinforcement, which allowed load transfer between the phases. The reinforcement with γ-Al_2O_3 - metal oxide created higher strength than that with Al_2O_3 (1-10 μm, platelet, α-phase) - metal oxide, caused

by the recrystallization effect of the secondary alumina phase in reticular-form after sintering (Fig. 4.10(b)). Although in the same percent of additives, the reinforcement by the nanocrystalline Al_2O_3 (10-100 nm, fibrous-shape, γ-phase) gives higher shrinkage than the Al_2O_3 (1-10 μm, platelet, α-phase) reinforced, this type of phenomena has been documented in topic 4.1. This difference may be result from the higher compaction degree during sintering of the materials and from the compatibility between the sizes of reinforced materials and ceramic matrix [167]**.** Especially the nanocrystalline phase of the γ-Al_2O_3 and ZnO additives are related to the strength of the materials also. However, it was found that no strong difference in shrinkage between all materials in this study occurred.

In the same type of reinforcing materials, **group 11** (**D25-27**), the strength of all composites were found not statistical significant relatively with the different in the composition of additives. Although the nanocomposite structure formations, secondary phase of gahnite, and relative high amount of crystalline phase incremented the strength, but the enhancement may be reduced by the negative influence of the porosity. As expected, hardness in composites should decrease with decreasing alumina content, but the enhancement may increase by the new hard phases (e.g. gahnite and spinel) and reduced by the porosity. Indentation fracture toughness determinations were conducted on the densest composites. The K_{IC} exhibited an increasing trend with increasing ZnO content and these findings are similar to the outcomes reported by Duan et al. [108].

The fracture toughness of all Al_2O_3-M_xO_y reinforced porcelain ceramics was found to increase statistically significant compared with pure dental porcelain (Table 4.11). The toughness of all composite materials also exhibited a notable increase more

than 60%, varying from 1.01 MPa·$m^{1/2}$ (a value for dental porcelain) up to 2.61 MPa·$m^{1/2}$, as shown in Table 4.9. The higher toughness of all composite materials compared to dental porcelain is the result of the reinforcing second phase of alumina, gahnite, spinel and feldspar [104, 106]. Higher fracture toughness occurs oftener in two or more phase materials than in single-phase materials if the second reinforcing phase makes crack propagation more difficult, due to the formation of the crack requires higher energy [168]. The presence of rigid additives, alumina reinforcing phase and new phase formation, in these composite materials, and especially the nanocomposite structure formations, contributed to the high toughness.

All Al_2O_3-M_xO_y reinforced porcelain ceramics illustrated in Figs. 4.13 and 4.14 showed a good dispersion of reinforcing materials due to an adequate mechanical mixing. All composite materials showed altered structure of reinforced materials and were different from the parent reinforced materials. All of them, except **D23** and **D25**, had nanocomposite structure formation. The observations emphasize that the bending strength and toughening mechanism of materials are as described in topic 4.1. Although **D23** had no nanocomposite materials formation, the recrystallization of alumina from nanocrystalline phase into microcrystalline clusters and reticular-form causes the highest strength. In this study, undetected Al_2TiO_5 may be resulted from the unsuitable sintering condition or the low percentage of titania. Crystal and matrix microcracking have been linked to the phase transformation of alumina (cubic to rhombohedral) [169]. This effect made a resultant anisotropic stress distribution. A leucite particle also recommended to minimize microcracking in leucite containing dental porcelain is confirmed by the present work [10]. The different in thermal coefficient between types of reinforcement and new phase formation were proposed

to cause the development of residual tensile stresses in the matrix around the reinforcement from the rapid cooling of the sintering process [170].

A certain crack deflection effect was consequently expect, since cracks were thought to be attracted towards the reinforcement and propagate further through the rupture of the glass matrix-reinforced material interface. The fracture propagation in the composites would be consequently more difficult than in the pure dental porcelain. The crack deflection mechanism was found to be effective, since the roughness of the fracture surfaces of the composite materials were relevant, in good agreement with the findings in the literature [10]. The crack deflection effect was confirmed by the observation of the crack pattern developed by Vickers indentation, as shown in Fig. 4.16. The reinforcing ability of the crystalline phases and the effectiveness of crack deflection were confirmed by the hardness and toughness data (Table 4.9). The Weibull distributions are narrower for example **D23** and **D26** as would be expected as surface roughness. Flaw size and distribution have been shown the effect to the strength values. The Weibull *m*-values were improve over these materials, in good agreement with the comparable strength probabilities of failure (Table 4.11 and Fig. 4.18).

X-ray diffraction of dental porcelain (Fig. 4.11) and all Al_2O_3-M_xO_y reinforced porcelain ceramics (Figs. 4.11 and 4.12) showed that the beam deflected from random oriented crystals. The alignment of reinforcing crystalline phase and nanocomposite structure formation in some conditions occurred in the materials perpendicular to these crystals, resulting in the higher fracture toughness. The XRD analysis of all Al_2O_3-M_xO_y reinforced porcelain ceramics showed that a considerable amount of new crystalline phase was already transformed in the as-sintered materials. The new phase

formation of spinel and gahnite from the metal oxide added in the **D24-D27**, following the reactions:

$$Al_2O_3 + MgO \longrightarrow MgAl_2O_4 \quad (1)$$

$$Al_2O_3 + ZnO \longrightarrow ZnAl_2O_4 \quad (2)$$

The greater amount of gahnite was detected on the **D27** and related with the amount of ZnO added. The error resulting from using the XRD analysis to measure the amount of the crystalline phase from the specimens is relatively high. However, these results are correlated to the ease of new phase formation and suggest that they contributed to the fracture toughness. The amount of crystalline phase can be related to the transformation toughening mechanisms, which were expected to be considerably. More effective these composite materials due to the magnitude of the new phase transformation, the lack of the glassy phase.

This section demonstrates that the strength of dental porcelain ceramics can be significantly enhanced by employing a combination between the Al_2O_3-M_xO_y reinforcement and the nanocomposite approach. However, some other factors such as porosity, morphology, secondary phase formation and orientation of crystalline phase, are also important in determining the mechanical properties of materials.

The last remarkable, for the comparative all flexural strength and porosity data in this chapter can be summarized in Fig. 4.19.

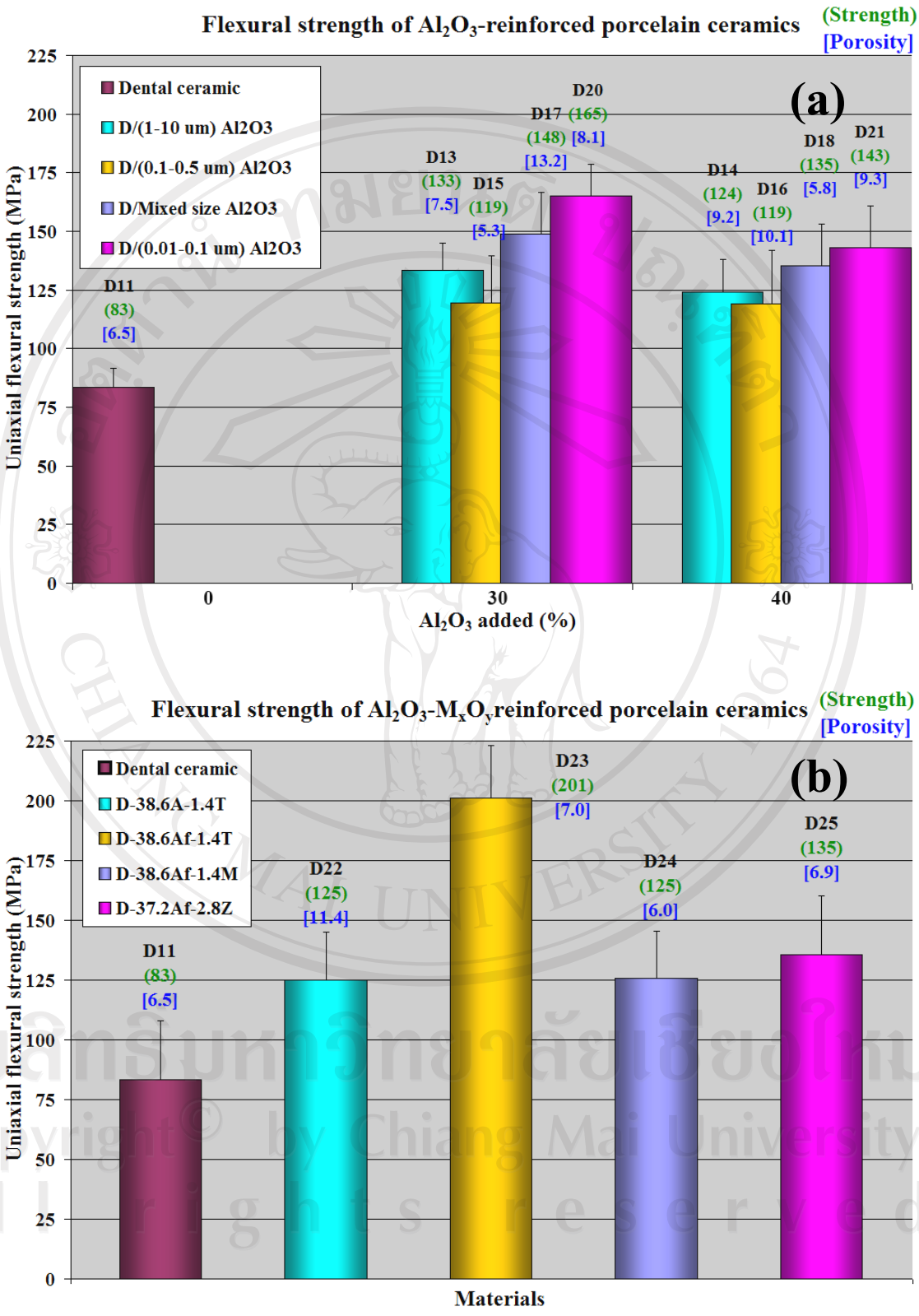

Fig. 4.19 The comparative all flexural strength and porosity data of (a) Al_2O_3 and (b) Al_2O_3-M_xO_y reinforced porcelain ceramics.